Observation of fast time scale spectral diffusion in a low temperature glass: comparison of picosecond photon and stimulated echoes

L.R. Narasimhan [1], Y.S. Bai [2], M.A. Dugan and M.D. Fayer
Department of Chemistry, Stanford University, Stanford, CA 94305, USA

Received 18 September 1990; in final form 21 October 1990

Results of temperature-dependent two-pulse photon echo and three-pulse stimulated echo experiments on an organic dye (rhodamine 101) in a polymer glass (PMMA) are presented. Decay rates at a fixed temperature are shown to increase as the waiting time, T_w (time between the second and third pulse) of the stimulated echo increases. This is due to spectral diffusion caused by structural relaxations of the host. At a fixed waiting time, decay rates follow a power law dependence on temperature which is characteristic of the glassy state. The data are analyzed by explicitly evaluating the stimulated echo correlation function for short T_w.

1. Introduction

Optical dephasing (line narrowing) measurements have been used extensively to study dynamics in condensed matter systems [1–4]. Various techniques have been developed to permit the extraction of line widths and subtle spectral features from media whose absorption spectra are dominated by inhomogeneous broadening. These data have then been used to infer dynamical information of the systems under study [1–14]. More recently, several workers have pointed out that in complex systems such as spin-active crystals [15,16] and glasses [11–14], different dephasing techniques will not, in general, yield the same dynamical observable, the homogeneous line width. Each method (photon echo, hole burning, etc.) is sensitive to a range of relaxation rates in the medium or, alternatively, there is a characteristic time scale associated with each measurement [9,13,17,18]. The two-pulse photon echo, for example, is sensitive to fast rates on the order of the separation between the excitation pulses (ps to ns) while hole burning is sensitive to all processes which occur between burning and reading of the hole (μs to days) [11–14,15,16,19,20]. In the case of glasses, which are known to evolve structurally over long times, the line width obtained by hole burning will be broader than that from the photon echo [11–13,19]. This difference is usually termed spectral diffusion.

Various low temperature anomalies in glasses (e.g. excess heat capacities [21], unusual thermal conductivities [21], etc.) have been successfully explained with the tunnelling two-level system (TLS) model proposed by Phillips [22] and Anderson, Halperin and Varma [23]. Here, the multidimensional glass potential surface is modelled as a distribution of asymmetric double wells (two-level systems or TLS), each characterized by an energy splitting, E, and a tunnelling parameter, λ. Each well represents some distinct local configuration of the glass molecules. For E and λ having broad distributions, a fluctuation rate distribution for the medium, $P(R)$, is obtained which spans a very wide range of rates. Determining $P(R)$ is, therefore, a key problem in understanding the behavior of low temperature glasses. Studying complex systems with a variety of different

[1] Present address: AT&T Bell Laboratories, Murray Hill, NJ 07974, USA.
[2] Present address: SRI International, Menlo Park, CA 94025, USA.

0009-2614/91/$ 03.50

dephasing techniques can and has provided dynamical information on solute–solvent interactions [11,12] and fluctuation rate distributions [11–18] which cannot be obtained with any one method.

In this article we report the results of two-pulse photon and three-pulse stimulated echo experiments on rhodamine 101 in a PMMA glass. In the case of the three-pulse echo, the time between pulses 2 and 3 (T_w) is kept fixed, and the delay between pulses 1 and 2 (τ) is scanned. This yields a decay which is sensitive to both fast processes (homogeneous dephasing) as well as spectral diffusion. An analysis of the four-time correlation function of the stimulated echo is given in the short waiting time limit to evaluate the data. This is necessary because past treatments of the problem have been for the limits of either zero waiting time (two-pulse echo) [24] [#1] or very long waiting times (hole burning) [13,17,18]. The data are shown to be consistent with a fluctuation rate distribution $P(R) \propto 1/R$ which has been reported for a variety of other low temperature glasses based on line shape arguments [11–14].

2. Experimental procedures

The laser system used in these experiments has been described in detail elsewhere [4]. It is an amplified sync-pumped dye laser capable of producing 4 ps, near transform limited pulses of approximately 1.5 μJ at a 1 kHz repetition rate. The experimental apparatus is shown in fig. 1 and is capable of generating both two- and three-pulse echoes. The amplified pulse passes through a variable attenuator and is split with a 30% beamsplitter. The through beam (beam 1) goes to a continuously scannable delay line consisting of a corner cube on a precision stepper motor (Aerotech Corp.) both of which sit atop a precision optical rail (Gaertner Corp.) capable of scanning long delays. This delay line was double-passed with a roof prism. The reflected beam from

[#1] Note that there is an error in a numerical integral in ref. [24]. The value reported as 2.63 should be 3.66.

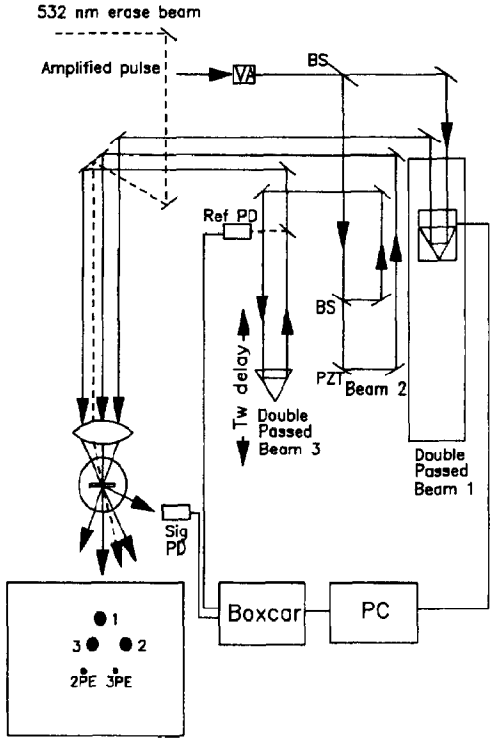

Fig. 1. Apparatus used to perform two-pulse photon and three-pulse stimulated echoes. VA=variable attenuator, BS=beamsplitter, PZT=piezo-electric transducer, PD=photodiode. The inset shows the location of the signals relative to the input beams.

the beamsplitter (beam 2) passed down a fixed delay and reflected off of a pair of mirrors, one of which is mounted on a piezo-electric transducer (PZT). This aided in the investigation of possible accumulation effects. Beam 2 is then split to generate beam 3 which could be delayed with respect to beam 2 via another double-passed delay line. This delay line was not continuously scannable but the corner cube could be manually moved to various positions. In this scheme, the scannable delay, τ, was between the first two beams and T_w is the delay between beams 2 and 3.

All three beams may be overlapped in time if necessary to aid in locating the signal. The maximum possible τ delay was 12 ns while the maximum possible T_w was 9 ns, but these limits were not reached during the course of the measurements. The three beams were gently focused into the sample with a 60 cm lens which yielded a spot size of approximately 200 μm determined by putting the beams through a pinhole at the focus. Care was taken to ensure that all three beams underwent the same number of reflections through the course of the various delays. This ensured that overlap would be maintained regardless of pointing fluctuations. With this apparatus, it was possible to measure the three-pulse stimulated echo and then, simply by blocking beam 3, the two-pulse echo on the same spot in the sample without any realignment of the input beams. The crossing angle between beams 2 and 3 was approximately 2° and was slightly smaller than the angles between beams 1 and 3 and 1 and 2. The grating in frequency space which is characteristic of the stimulated echo was formed by beams 1 and 2. Pulse 3 scattered from this grating in a direction determined by phase matching and was subsequently detected by a fast photodiode and transimpedance amplifier. The data were collected with gated integrators and associated software which filters out points for which the input laser intensity fluctuated beyond preset limits (usually ±10%). This permitted running the delay line quickly since there was no time constant usually associated with lock-in detection. A scan of several nanoseconds delay in τ could be done within 30–40 s.

The samples of rhodamine 101 (Rh101) in PMMA were supplied by courtesy of Dr. Bernhard Dick (Max-Planck-Institut für Biophysikalische Chemie, Göttingen, Germany). They were prepared by direct polymerization of a dye–polymer mixture [25]. The polymerization was carried out over a period of two weeks after which slices were cut and polished for use. The samples were of very good optical quality and physically uniform. After mounting on a copper block, the samples were placed in a liquid helium dewar and studied over the temperature range 1.1–2.1 K. In all cases, the samples were immersed in superfluid liquid helium and the temperature was controlled by maintaining the vapor pressure over the liquid helium (Barocel Corp. capacitance manometer). Temperature regulation was within ±0.05 K. A pinhole was mounted in the same plane as the sample. Before each series of experiments, the spots were crossed at this point and the delay line alignment checked carefully to ensure that the spot size of the scanned beam does not change and that the scanned beam did not spatially deviate. These conditions were periodically checked during each experimental run. The excitation wavelength was typically 596 nm and color dependences showed no variations in decay times within $\tau\eta\epsilon$ ±3 nm studied. The availability of the third beam also permitted measurement of the lifetime of the dye (T_1) via the transient grating technique [26]. This was done by making beams 2 and 3 time coincident, scanning beam 1, and looking in a different phase matched direction. The lifetime is 3.4 ±0.2 ns.

Although PMMA has a much lower hole burning efficiency than hydrogen bonded glasses such as ethanol, some slight hole burning was noticed over several scans. This requires the ability to fill holes burned during the duration of a scan. Rebane and Haarer [27] have reported that hole filling may be induced by exposing an irradiated spot to high intensity white light for several minutes. We found that exposing the spot for a few seconds to approximately 100 mW of 532 nm light fills in even very deep holes. These data were collected by filling the hole after each scan for 30 s and then letting the sample re-equilibrate for 90 s afterwards. This hole filling method was recently exploited by Littau and Fayer in a fast time resolved hole burning study on the cresyl violet/deuterated ethanol system [20].

3. Results

Fig. 2 shows a two-pulse echo ($T_w=0$) and a three-pulse echo ($T_w=2$ ns) on the Rh101/PMMA system at 2.05 K. These and other decays were studied as a function of power and were obtained with pulse energies of approximately 100 nJ/pulse. In this regime, no variation of decay time with pulse energy was observed, and in fact, no variation was observed at the highest available energies. As mentioned previously, hole burning effects during any one scan were small but could accumulate over prolonged signal averaging periods, causing the signal intensity to gradually decrease because of burning. The 30 s fill, 90 s wait cycle after each scan was adopted to counteract these effects. Hole filling opens up many new possibilities for studying systems such as ethanolic glasses which undergo very rapid hole burning [11–14,20]. A calculation [28] showed that if the hole is completely filled after each sweep, the hole burning effect cancels when the average of a number of forward and backward scans is taken. Signal-to-noise ratios such as those shown in fig. 2 were readily obtained 8 to 10 scans for the two-pulse echo and 20 scans for T_w approaches 3 ns. Two-pulse echoes taken with the third beam on agreed with those taken with the third beam blocked. As T_w increased beyond the fluorescence lifetime, the signal intensity of the three-pulse echo dropped dramatically, as expected. The signal was detectable by eye at $T_w=3$ ns (using full laser power) where it was slightly less intense than the adjacent two-

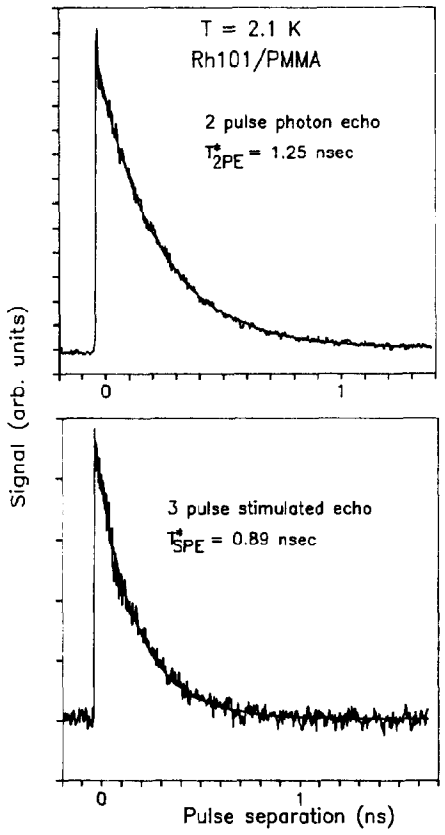

Fig. 2. Comparison of two-pulse photon echo ($T_w=0$) and three-pulse stimulated echo ($T_w=2$ ns) in Rh101/PMMA at 2.1 K. The stimulated echo is approximately 35% faster than the two-pulse echo as a result of spectral diffusion in the polymer glass. The solid lines are fits to an exponential.

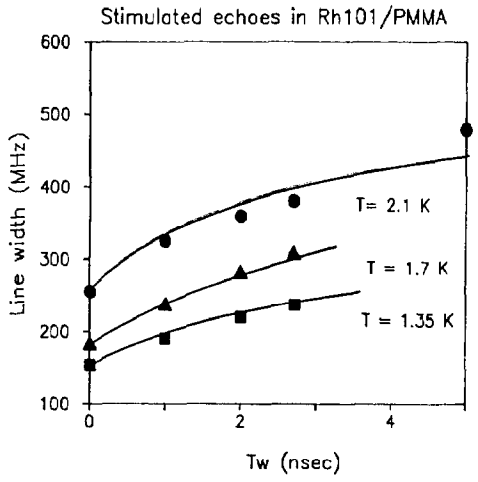

Fig. 3. Temperature- and waiting-time-dependent study of two- and three-pulse echoes in Rh101/PMMA. The decay times are plotted as lifetime corrected line widths (see text). Line widths increase with temperature and T_w. The solid lines are predicted values for the line widths based on an analysis of the stimulated echo correlation function for short waiting times.

pulse echo (at time $\tau=0$). Beyond this waiting time, the signal could only be found through scattering from an accumulated grating [29]. Rh101 has a long-lived bottleneck with an approximately 1 s lifetime at low temperatures. At $T_w=5$ ns, it was possible to see the signal build up to a steady state value after unblocking the beams. Dithering the PZT destroyed the accumulation effect by destroying the phase coherence between pulses 1 and 2. Accumulation did not occur while scanning the delay line, therefore any effect that accumulation would have on the decay time was eliminated.

Although excitation occurred well to the red of the absorption maximum, there was a contribution to the short time (few ps) decays due to excitation of phonons as well as from a coherent peak. The long tail reflects the dephasing of the zero-phonon line [10] and could be fitted to an exponential. Decays were fitted (excluding the short time behavior) with a non-linear least-squares algorithm. Results of a temperature- and waiting-time-dependent study on Rh101/PMMA are shown in fig. 3. Clearly, the decay times change as a function of T_w which is a direct result of spectral diffusion. The data shown are given as line widths, Γ, obtained through the relation, $\Gamma=1/\pi T^*_{2PE,SPE}$. $T^*_{2PE,SPE}$ is the lifetime corrected dephasing time measured by the two-pulse echo (2PE) or stimulated echo (SPE). The change between $T_w=0$ and $T_w=2$ ns is approximately 35%. Only one point at $T_w=5$ ns is shown. The two-pulse echo decays could be fitted to the characteristic power law temperature dependence seen in many glassy systems: $\Gamma\propto T^{1.3-1.4}$ [1-8,11-14].

4. Analysis of short waiting time dephasing

Here, we address the theoretical problem of dephasing measurements with a view towards determining the form of the fluctuation rate distribution from the data in fig. 3. In general, this involves averaging the four-time correlation function which describes the stimulated echo experiment, over the glass parameters, i.e. the dye–glass coupling and the stochastic path histories of the fluctuating TLS. Hu and Walker [30] analyzed spectral diffusion decays in magnetic resonance problems by taking the average of spin flip histories based on an uncorrelated sudden jump model for a single rate, R, in the Laplace domain and then inverting back into the time domain. In our case, this corresponds to independent TLS tunnelling events. For the case of dipolar coupling, they derive the result (eq. (15) of ref. [30])

$$f(2\tau, T_w)\rightarrow \frac{2w_1w_2}{(w_1+w_2)^2}\frac{2(w_1+w_2)+\sigma\{1-\exp[-(w_1+w_2)T_w]\}}{\{[\sigma+2(w_1+w_2)](\sigma+2w_1)(\sigma+2w_2)\sigma^3\}^{1/2}}, \tag{1}$$

where w_1 and w_2 are the up and down transition rates and the arrow indicates that the right-hand side is in the Laplace domain while the left-hand side is in the time domain. Given $w_1/w_2=\exp(-E/kT)$ and $w=w_1+w_2$ ($\equiv R$), this yields

$$f(2\tau, T_w)\rightarrow \mathrm{sech}^2(E/2kT)\frac{2w+\sigma[1-\exp(-wT_w)]}{\{\sigma^3(\sigma+2w)\{\sigma+2w/[1+\exp(-E/kT)]\}\{\sigma+2w/[1+\exp(E/kT)]\}\}^{1/2}}. \tag{2}$$

Under these conditions the transform can be inverted analytically to give [30]

$$f(2\tau, T_w)=\frac{2w_1w_2}{(w_1+w_2)^3}\{F(\xi;w\tau)+[1-\exp(-RT_w)]G(\xi;w\tau)\}, \tag{3}$$

with $\xi=(w_1-w_2)/(w_1+w_2)$ and the F and G are defined as integrals over modified Bessel functions. This problem has been treated in the $T_w=0$ limit by Maynard, Rammal, and Suchail [24] and in the long waiting time limit ($T_w\gg 10\tau$) by Bai and Fayer [17,18]. Maynard et al. studied the F function for a *distribution* of spin flip rates with dipolar coupling and showed that an exponential decay resulted from a $1/R$ ($1/w$ in the Hu and Walker notation) distribution. Bai and Fayer analyzed a variant of the G function in refs. [17,18]. Their F_2 function is analogous to G and their F_1 function is analogous to F. F_1 contributes on the photon echo time scale (fast rates). F_2 is waiting time independent but, when multiplied by the factor $[1-\exp(-RT_w)]$

yields a function whose width depends on T_w. Bai and Fayer then showed that for $T_w \gg 10\tau$, F_2 is the dominant contributor to measured dephasing and that regardless of the form of the rate distribution, dipolar coupling will yield exponential decays of the correlation function (Lorentzian lines in hole burning measurements). This result is consistent with the less general results of other workers [9]. It is possible to use these methods to extract rate distributions from measured changes in long time line widths, and they have been applied with success to a number of different systems [14,18,20].

In the case of the three-pulse stimulated echo for relatively short T_w, there will be a contribution to the decay of the correlation function from both F_1 and F_2 and this must be considered explicitly. Furthermore, the approximations used by Bai and Fayer in the evaluation of F_2 in the long waiting time limit are not valid for short T_w. The observation of exponential two-pulse echoes suggests that a $P(R) \propto 1/R$ distribution is a good starting point in analyzing the data presented here. The average of the waiting-time-dependent part of eq. (2) is

$$\frac{1}{2\sigma^2}\int_0^\infty dx\,\mathrm{sech}^2(x/2)\int_0^\infty \frac{[1-\exp(-RT_w)]\,dR}{R\{(1+2R/\sigma)\{1+2R/\sigma[1+\exp(x)]\}\{1+2R/\sigma[1+\exp(-x)]\}\}^{1/2}}, \tag{4}$$

where $x=E/kT$. We evaluate this integral numerically, add it to the waiting-time-independent component to obtain the total history average in the intermediate time and dipolar coupling case. A program based on the Stehfest algorithm [31] inverts the average back into the time domain. The correlation function is obtained by taking the exponential of minus the average and the signal is proportional to the square of the correlation function. (Note that in the $T_w=0$ case, the waiting-time-dependent portion of the history average disappears and furthermore, the two-pulse echo function, F_1, simply evaluates to $3.66/\sigma^2$. When inverted back into the time domain, this gives a constant times the pulse separation, τ. This results in the observed exponential two-pulse echo decay.) All of the computations were performed on a Digital Equipment Corporation Decstation 3100 workstation using programs written in C.

The results of the calculations of the signal for different waiting times are given in semi-logarithmic form in fig. 4. The curves for $T_w > 0$ predict non-exponential decays. The detected signal is proportional to the square of the correlation function and typically 4–5 factors of e decay are seen (2–2.5 factors of e decay of the correlation function). In this range, the correlation function decay can be fitted to a straight line by a linear regression algorithm and the deviations from exponential would be hard to see given normal experimental signal-to-noise ratios. Furthermore, actual echo decays can only be fitted for pulse separations greater than approx-

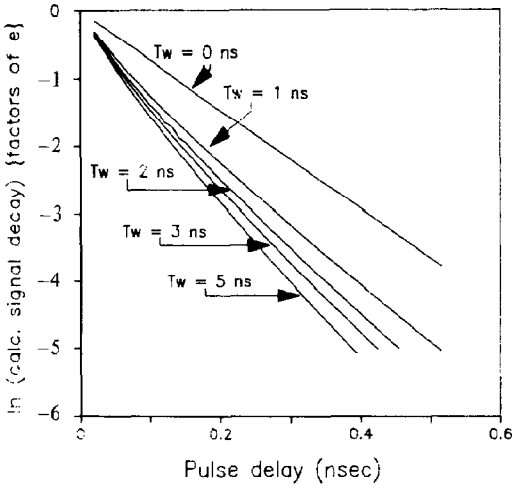

Fig. 4. Semilog plot of the calculated stimulated echo signal as a function of T_w. The $T_w=0$ point represents the photon echo decay, the straight line corresponds to an exponential decay of the measured signal. The finite waiting time correlation functions are strictly non-exponential. However, in the regime where data are obtained, they will be hard to distinguish from exponentials. The slopes of the finite waiting time correlation functions are ratioed to the slope of the two-pulse echo to determine the amount of broadening due to spectral diffusion.

imately 30 ps because of the short time contributions from the coherent peak and phonons discussed in section 3. The T_w-dependent theoretically calculated slopes for times longer than 30 ps were ratioed to the two-pulse echo case to determine the amount of broadening. The data in fig. 3 are shown with solid lines predicted by the results of this analysis with no adjustable parameters. The only input is the decay constant determined by the two-pulse echo measurement. The agreement is good to within the scatter of the data and the slight uncertainty in determining the slopes of the calculated curves. We conclude, therefore, that the $P(R) \propto 1/R$ distribution is consistent for rates from approximately 1/0.5 ns to 1/5 ns.

In a previous study of optical dephasing in PMMA [32], in which the chromophore was rhodamine B, the temperature dependence of the photon echo decay was found to be a power law at low temperature with an exponentially activated contribution becoming important above 5 K. This is consistent with previous observations on other systems [4]. Rhodamine 101 is very similar to rhodamine B. In this study, the temperature dependence was examined only at low temperatures (<2.15 K). In this range of temperatures, the observed power law ($T^{1.3-1.4}$) demonstrates a distribution of energies of the TLS, $P(E) \propto E^{0.3-0.4}$ [9]. Within the TLS model, the observed $1/R$ rate distribution and the almost flat distribution of energies suggests a flat or close to flat distribution of the tunnelling parameter, $P(\lambda)$.

5. Conclusions

We have presented results of temperature- and waiting-time-dependent echo experiments on a polymeric glass between 1.1 and 2.1 K. The measured decay times decrease with increased waiting time, T_w, providing direct evidence of fast spectral diffusion in this material. Decay rates also increased with increasing temperature in a manner consistent with other dephasing measurements on glassy systems [6,7,11–14]. The data are analyzed by explicitly considering the history average of the stimulated echo correlation function in the short T_w case. A good fit to the data can be obtained by assuming a rate distribution $P(R) \propto 1/R$ for the range of rates probed by the experiment, $1/0.5 \text{ ns} > R > 1/5$ ns. Given the almost linear temperature dependence, $P(R)$ can be used to infer the distribution of tunnelling parameters of the two-level systems. This technique and the associated theoretical treatment in conjunction with other dephasing measurements on faster and slower time scales are useful in quantifying the behavior of complex systems such as low temperature glasses which are one important example.

Acknowledgement

This work was supported by a grant from the National Science Foundation, Division of Materials Research (No. DMR87-18959). Additional support was provided by the Office of Naval Research, Physics Division (No. N000014-89-J1119). The DEC computers were funded by a Computing Grant from the National Science Foundation (No. CHE 88-21737). LRN thanks the Fannie and John Hertz Foundation for a graduate fellowship. We wish to thank Dr. Bernhard Dick for the gift of the polymer samples, S. Greenfield for his help with the data collection software, R. Dorfman and Professor J. Najbar for useful discussions on numerical algorithms, and D. Zimdars for technical assistance.

References

[1] J. Luminescence 36 (1987), Special Issue.
[2] W.E. Moerner, ed., Persistent spectral hole burning: science and applications (Springer, Berlin, 1988).
[3] R. Jankowiak and G.J. Small, Science 237 (1987) 618.

[4] L.R. Narasimhan, K.A. Littau, D.W. Pack, Y.S. Bai, A. Elschner and M.D. Fayer, Chem. Rev. 90 (1990) 439.
[5] A. Elschner, R. Richert and H. Bassler, Chem. Phys. Letters 127 (1986) 105.
[6] R. Jankowiak, L. Shu, M.J. Kenney and G.J. Small, J. Luminescence 36 (1987) 293.
[7] R.H. van den Berg and S. Völker, Chem. Phys. 128 (1988) 257.
[8] K.K. Rebane and L.A. Rebane, in: Persistent spectral hole burning; science and applications, ed. W.E. Moerner (Springer, Berlin, 1988) ch. 2.
[9] D.L. Huber, M.M. Broer and B. Golding, Phy. Rev. Letters 52 (1984) 2281;
W.O. Putikka and D.L. Huber, Phys. Rev. B 36 (1987) 3436.
[10] S. Saikan, T. Nakabayashi, Y. Kanematsu and N. Tato, Phys. Rev. B 38 (1988) 7777.
[11] D.W. Pack, L.R. Narasimhan and M.D. Fayer, J. Chem. Phys. 92 (1990) 4125.
[12] L.R. Narasimhan, D.W. Pack and M.D. Fayer, Chem. Phys. Letters 152 (1988) 287.
[13] M. Berg, C.A. Walsh, L.R. Narasimhan, K.A. Littau and M.D. Fayer, J. Chem. Phys. 88 (1988) 1564.
[14] K.A. Littau, Y.S. Bai and M.D. Fayer, J. Chem. Phys. 92 (1990) 4145.
[15] R.M. Shelby and R.M. Macfarlane, J. Luminescence 31/32 (1984) 839.
[16] R.M. Shelby and R.M. Macfarlane, J. Luminescence 36 (1987) 179.
[17] Y.S. Bai and M.D. Fayer, Commun. Cond. Matt. Phys. 14 (1989) 343.
[18] Y.S. Bai and M.D. Fayer, Phys. Rev. B 39 (1989) 11066.
[19] W. Breinl, J. Friedrich and D. Haarer, J. Chem. Phys. 81 (1984) 3915.
[20] K.A. Littau and M.D. Fayer, Chem. Phys. Letters, submitted for publication.
[21] W.A. Phillips, ed., Amorphous solids: low temperature properties (Springer, Berlin, 1981).
[22] W.A. Phillips, J. Low. Temp. Phys. 7 (1972) 351.
[23] P.W. Anderson, B.I. Halperin and C.M. Varma, Phil. Mag. 25 (1972) 1.
[24] R. Maynard, R. Rammal and R. Suchail, J. Phys. (Paris) 41 (1980) L291.
[25] B. Dick, Chem. Phys. 136 (1989) 429.
[26] M.D. Fayer, Ann. Rev. Phys. Chem. 33 (1982) 63.
[27] A. Rebane and D. Haarer, Chem. Phys. Letters 70 (1989) 478.
[28] D. Zimdars, private communication.
[29] W.H. Hesselink and D.A. Wiersma, J. Chem. Phys. 73 (1980) 648.
[30] P. Hu and L.R. Walker, Phys. Rev. B 18 (1979) 1300.
[31] H. Stehfest, Commun. ACM 13 (1970) 47.
[32] A. Elschner, L.R. Narasimhan and M.D. Fayer, Chem. Phys. Letters 171 (1990) 19.